ELSEVIER
Available online at www.sciencedirect.com
SCIENCE DIRECT®
Advances in Space Research xxx (2005) xxx–xxx
ADVANCES IN SPACE RESEARCH
(a COSPAR publication)
www.elsevier.com/locate/asr

Signatures of the nightside open–closed magnetic field-line boundary during moderately disturbed conditions and ionospheric substorms

M.L. Parkinson [a,*], M. Pinnock [b], P.L. Dyson [a], J.C. Devlin [c]

[a] Department of Physics, La Trobe University, Bundoora Campus, Melbourne, Vic. 3086, Australia
[b] British Antarctic Survey, Natural Environment Research Council, Cambridge CB3 0ET, UK
[c] Department of Electronic Engineering, La Trobe University, Melbourne, Vic. 3086, Australia

Received 19 October 2002; received in revised form 8 June 2005; accepted 20 June 2005

Abstract

The comparatively low latitude of the Tasman International Geospace Environment Radar (TIGER) (147.2°E, 43.4°S, geographic; −54.6°Λ), a Southern Hemisphere HF SuperDARN radar, facilitates the observation of extensive backscatter from decametre-scale irregularities drifting in the auroral and polar cap ionosphere in the midnight sector. The radar often detects a persistent, sharp increase over ∼90 km of range in line-of-sight Doppler velocity spread, or spectral width, from <50 m s^{-1} at lower latitude to >200 m s^{-1} at higher latitude. It was previously shown that for moderately disturbed conditions in the pre-midnight sector, the location of the spectral width boundary (SWB) corresponds to the poleward edge of the auroral oval determined using energy spectra of precipitating particles measured on board Defense Meteorology Satellite Program satellites. This implies the radar SWB is a proxy for the open–closed magnetic field-line boundary (OCB) under these particular conditions. Here we investigate whether the radar SWB is aligned with the satellite OCB under a broader range of geomagnetic conditions including small to moderate substorms occurring in the pre- and post-magnetic midnight sectors. The behaviour of the SWB can be reconciled with the spatial and temporal variations of energetic particle precipitation throughout the substorm cycle.

Keywords: Ionospheric substorms; Magnetic field lines; Geomagnetic condition; Open–closed magnetic field-line boundary

1. Introduction

The Super Dual Auroral Radar Network (SuperDARN) presently consists of 17 HF backscatter radars, each with a similar design optimised to measure ionospheric convection on a global scale (Greenwald et al., 1995). The radars employ phased antenna arrays to sequentially step the main beam through 16 directions separated in azimuth by 3.24° to from 52°-wide scans. Each radar records echo parameters, including the backscatter power, line-of-sight Doppler velocity, and Doppler velocity spread (or "spectral width"), once every 1–2 min on up to 70 ranges between 180 and 3330 km in 45-km steps. The spectral widths are a measure of space and time variations in the line-of-sight velocity occurring within the sampling volume and integration time.

A sharp increase in the spectral widths from <50 m s^{-1} at lower latitude to >200 m s^{-1} at higher latitude is often observed in the dayside ionosphere, and has been interpreted as a proxy for the open–closed magnetic field-line boundary (OCB) when the interplanetary magnetic field (IMF) B_z component is southward (Baker et al., 1995). A similar spectral width boundary (SWB) is often observed in the nightside ionosphere, and it seems natural to consider whether it may also

* Corresponding author. Tel.: +61 3 94791433; fax: +61 3 94791552.
E-mail address: m.parkinson@latrobe.edu.au (M.L. Parkinson).

0273-1177/$30 © 2005 Published by Elsevier Ltd on behalf of COSPAR.
doi:10.1016/j.asr.2005.06.082

correspond to the OCB. An early case study suggested the nightside SWB was the boundary between the central plasma sheet (CPS) and the so-called boundary plasma sheet (BPS) (Dudeney et al., 1998). However, recent studies show the SWB is often a reasonable proxy for the OCB in the dusk and midnight sectors (Lester et al., 2001; Parkinson et al., 2002; Chisham and Freeman, 2004). Parkinson et al. (2004) and Chisham et al. (2005) discussed the relation between energetic particle precipitation and the location of the SWB.

The purpose of this paper is to further investigate the relationship of the nightside SWB to magnetospheric boundaries under a broad range of geophysical conditions. For example, does the alignment of the SWB with the OCB change with MLT and geomagnetic activity? Does the SWB agree with the OCB during ionospheric substorms? Down to what spatial and temporal scales is the SWB an accurate proxy for the OCB? These are important questions to address because using SuperDARN observations to specify the location and shape of magnetospheric boundaries is a potentially valuable contribution to the wider space science effort.

2. Experiment

Because the Tasman International Geospace Environment Radar (TIGER) is one of the most equatorward of the SuperDARN radars ($-54.6°\Lambda$), it routinely detects the SWB in the midnight sector during moderately disturbed conditions and substorms. Here we analyse observations made during the two representative nights, September 5 and October 31, 2000. Range-time plots of spectral widths for the magnetic meridian pointing beam 4 are shown because full-scan observations confirm the midnight SWB is roughly aligned in a zonal direction, and thus will be sharper and more accurately located using an orthogonal beam. The SWB was automatically identified as the poleward edge of the most equatorward range cell with spectral width $<200\ \mathrm{m\ s^{-1}}$, whilst the next two range cells had a spectral width $\geqslant 200\ \mathrm{m\ s^{-1}}$, and the subsequent two range cells had spectral widths $\geqslant 100\ \mathrm{m\ s^{-1}}$. These conditions ensured the SWB was a well-defined feature in the data.

Dynamic energy spectra and pitch-angle distributions of precipitating particles at the poleward edge of the auroral oval are well known to indicate the location of the OCB (Vampola, 1971). Here we use nightside auroral oval boundaries determined using the logical criteria of Newell et al. (1996) applied to energy spectra of precipitating particles measured on board the Defense Meteorology Satellite Program (DMSP) satellites. Using the Newell et al. nomenclature, the most equatorward of the electron (b1e) or ion boundaries (b1i) was taken as the equatorward boundary of the auroral oval, and the most poleward of the electron (b5e) or ion boundaries (b5i) was taken as the poleward boundary. Strictly, though, the b6 boundary is the OCB. The boundary b4s is the "structured/unstructured boundary," considered here to be the boundary between the diffuse and discrete ovals. These auroral oval locations are superimposed as bold, vertical lines in subsequent range-time plots.

During the study intervals energy spectra were available from the four DMSP satellites, F12, F13, F14, and F15. Each satellite was in a Sun-synchronous, or fixed local time orbit. This meant there were only one or two auroral oval passes mapping to the radar field of view per night, including conjugate passes in the Northern Hemisphere. To extend the temporal coverage of boundary identifications, the Starkov (1994) statistical model of auroral oval boundaries was used to extrapolate the DMSP boundaries to the longitude of the radar measurements. However, the instantaneous auroral oval is unlikely to conform to any statistical model, especially during the expansion phase of substorms. To limit the magnitude of possible errors, the extrapolation was only applied to DMSP nightside boundaries identified within 2 h of the beam 4 longitude (i.e. $147.2° \pm 30°$E). Note that for September 5 and October 31, the average and standard deviation of the magnitude of corrections applied to the DMSP poleward edges were $0.9° \pm 1.0°\Lambda$ and $1.1° \pm 1.0°\Lambda$, respectively.

Three errors were involved in comparing DMSP and radar boundaries: (1) the error in mapping the DMSP measurements to magnetic latitude, probably $<0.5°$, (2) the error in mapping the radar scatter from group range to magnetic latitude, probably $<1°$, and (3) the error in extrapolating the DMSP boundaries to the longitude of the radar, probably $<2°$. Hence, adding these errors in quadrature, $\sqrt{5.25°} \approx 2.3°$ is a rough estimate of the maximum, conceivable error when comparing the OCBs with the SWBs.

3. Results

Fig. 1 is a summary plot of the observations made during the evening of September 5, 2000. Part (a) shows Macquarie Island (MQI) fluxgate magnetometer *perturbations* in the geomagnetic X (North), Y (East), and Z (down) components. These were calculated by transforming the absolute values to corrected geomagnetic coordinates, and then subtracting the daily means to facilitate comparison with the radar measurements. MQI (54.5°S,158.9°E; $-65°\Lambda$) is located just east of the TIGER field of view, and provides the most relevant measure of local auroral electrojet (AE) activity. Two small substorms occurred during this evening, with the ratio of Z to X perturbations indicating mostly westward current flow just poleward of MQI. The onset (O) of the first substorm occurred at 1402 UT, the peak expansion phase (P) at 1430 UT (~ -119 nT), and the recovery phase ended (R) at ~1633 UT. The onset of a second substorm occurred at 1659 UT. the peak expansion phase at 1813 UT (~−103 nT), and the recovery phase ended at ~1938 UT.

Fig. 1(b) shows the range-time plot of spectral widths measured along TIGER beam 4. Three different colours are used to represent three different kinds of echoes. The blue–grey colour represents sea echoes identified by "FITACF" (Baker, 1995), the standard algorithm used by all SuperDARN radars to analyse the autocorrelation functions of received signals. The purple colour represents ionospheric scatter with low spectral width <200 m s^{-1}. and the red colour represents ionospheric scatter with large spectral width ⩾200 m s^{-1}. As previously noted, the solid. fluctuating lines represent the automatically identified SWB, and the bold, vertical lines represent the corrected DMSP auroral oval locations. Horizontal bars are included to accentuate the locations of the equatorward and poleward edges, the latter indicating the OCB location.

Within experimental error, the SWB agreed with the OCB obtained from the F13 satellite pass at 1050 UT. This was near to when ionospheric scatter with low spectral width was located immediately equatorward of ionospheric scatter with large spectral width. However, the results indicate that prior to ~1250 UT the SWB was not aligned with the OCB. Some of the differences can be explained by considering the longitudinal separation between the radar and DMSP measurements (Parkinson et al., 2004). The SWB was poorly defined prior to 0930 UT, and after ~1050 UT there was no ionospheric scatter with low spectral width immediately equatorward of the SWB. Moreover, the next two DMSP auroral oval locations were also superimposed upon first-hop seas echoes (blue–grey). This suggests that an unobserved SWB may have actually occurred where the radar was observing first-hop sea echoes. Hence, the observed SWB may have been an artefact caused by leading edge, 1.5-hop rays entering the ionosphere in a region where large spectral widths extended much further equatorward. An examination of ionograms recorded at Hobart (−54°Λ) and MQI (−65°Λ) confirm that h_mF2, and hence the group delay to the apparent SWB, were increasing during ~1050 to 1250 UT.

Beyond 1250 UT there were more persistent ionospheric echoes with low spectral width immediately equatorward of the scatter with large spectral width. The OCB identified during the F15 satellite pass at 1320 UT agreed with the SWB. This identification occurred during the growth phase of the first substorm with onset at 1402 UT. The next two F13 satellite passes (1724, 1904 UT) were during the expansion and recovery

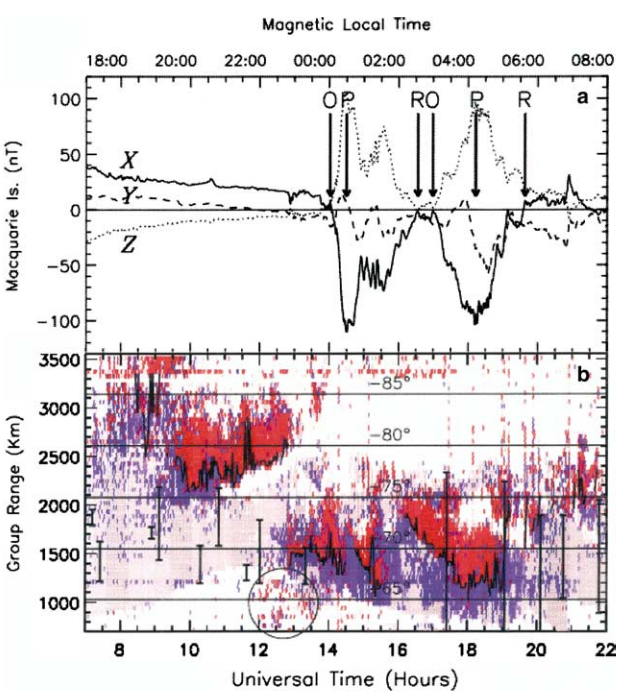

Fig. 1. (a) MQI magnetometer measurements of the geomagnetic X (solid), Y (dashed), and Z (dotted) perturbations at 1-min resolution during 07 to 22 UT on September 5, 2000. (b) Range-time plot of spectral width measured along TIGER beam 4. This is "common mode" data recorded with 2-min resolution per beam. The thin horizontal lines represent magnetic latitudes between −65° and −85°, and MLT is shown at the top of the figure. Other details are described in the text.

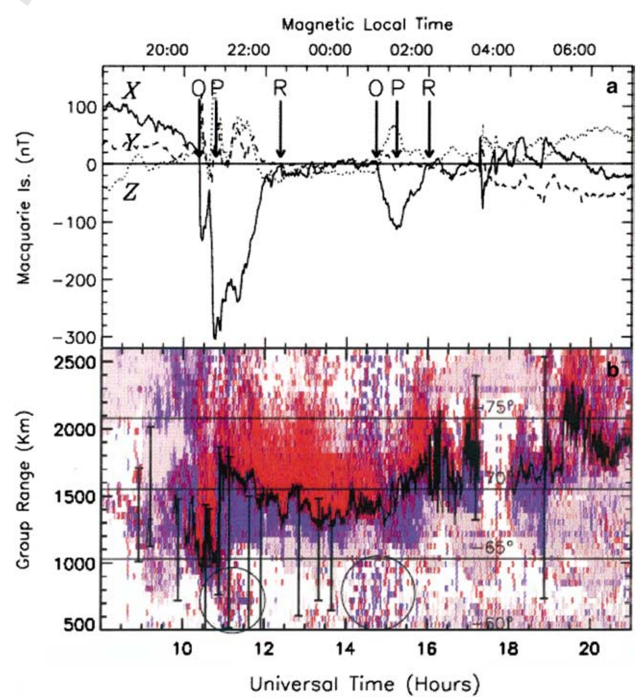

Fig. 2. (a) MQI magnetometer measurements of the geomagnetic X (solid), Y (dashed), and Z (dotted) perturbations at 1-min resolution during 08 to 21 UT on October 31, 2000. (b) Range-time plot of spectral width measured along TIGER beam 4. This is discretionary mode data recorded with 6-s resolution along beam 4. The results are presented in the same format as Fig. 1.

phases, respectively, of the second substorm with onset at 1659 UT. The boundaries between the discrete and diffuse aurora obtained from DMSP data were −66.4°Λ and −69.9°Λ, respectively, which better agreed with the SWB than the OCBs located ~7° further poleward. During this substorm observed in the morning sector the SWB was probably a better proxy for the poleward limit of energetic electron precipitation (Chisham et al., 2005). The OCB identified during the remaining three F13 passes beyond 06 MLT (2006, 2045, 2147 UT) all agree with the patchy SWB within experimental error. No substorm occurred during this interval.

Fig. 2 is a summary plot of the observations made during the evening of October 31, 2000. Part (b) shows the corresponding perturbations in the MQI geomagnetic *X*, *Y*, and *Z* components. Three substantial negative bays in the *X* component occurred during this evening. The onset (O) of a moderate substorm occurred at 1022 UT (~−330 nT), the peak expansion phase (P) at 1047 UT, and the recovery phase ended (R) at ~1222 UT. The relatively small amplitude of the *Z* component suggests the westward electrojet was centred above MQI (−65°Λ). The onset of a lesser substorm occurred at 1443 UT (~−118 nT), the peak expansion phase at 1513 UT, and the recovery phase ended at ~1601 UT. During this substorm the electrojet was located just poleward of MQI. Lastly, there was an impulsive increase in the *X* component at 1715 UT, immediately followed by an impulsive decrease, then a gradual increase. This sequence of events was initiated by the arrival of a dynamic pressure pulse in the solar wind. An analysis of this event is beyond the scope of this report.

Fig. 2(b) shows the range-time plot of spectral widths measured along TIGER beam 4, with annotations in the same format as Fig. 1(b). Prior to the onset of the first substorm at 1022 UT, there were small regions of large spectral width, but the SWB was poorly defined. Starting just prior to substorm onset and lasting until 1050 UT (just beyond peak expansion phase, 1047 UT), the radar measured ionospheric scatter with persistently large spectral width >200 m s^{-1} expanding equatorward to −64°Λ. Consequently, a well-defined SWB was identified during the expansion phase, in agreement with corrected DMSP OCBs identified by the F14 and F13 satellites (1033 and 1039 UT). The next four DMSP passes (1053, 1108, 1137, 1155 UT) were during the recovery phase ending near 1222 UT, and the poleward edges all agreed with the well-defined SWB within experimental error. Beyond the recovery phase the SWB fluctuated but trended equatorward, and the next three DMSP poleward edges (1251, 1320, 1339 UT) also agreed with the well-defined SWB.

A DMSP F 13 pass occurred at 1711 UT, just prior to the arrival of the dynamic pressure pulse at 1715 UT, with a subsequent outage of radar backscatter due to enhanced absorption. A final F 13 pass occurred at 1852 UT. In both cases the SWB was equatorward of the OCB. The boundary between discrete and diffuse aurora during these two passes were −72.4°Λ and −69.1°Λ, respectively, in reasonable agreement with the location of the observed SWB. However, the two OCBs were superimposed on 2nd-hop sea echoes (light grey), and the HF propagation conditions did not favour the detection of a SWB located that far poleward.

Full-scan data on September 05 (not shown) revealed an unusual population of intermittent ionospheric echoes with unusually large spectral width (>600 m s^{-1}), much larger than the spectral widths normally residing poleward of the fluctuating SWB. Other examples of these patchy echoes have been circled in Figs. 1(b) and 2(b). These echoes are thought to emanate from the polar cap, but are range folded echoes associated with the last pulse of a pulse set overlapping the subsequent pulse set (Greenwald, R., private communication).

4. Discussion and conclusions

For the TIGER radar the SWB is most likely to mark the ionospheric footprint of a magnetospheric boundary when the radar scatter is obtained via 0.5-hop HF propagation. Furthermore, the scatter showing low and high spectral widths should be unambiguously located in the upper *E* or *F* region of the ionosphere, since different plasma instabilities operate in the lower *E* region. It is also important for the SWB identification to be based upon observations of persistent ionospheric scatter with a well defined transition from low to high spectral widths. The September 05 event illustrated these aspects well. Prior to ~1250 UT high spectral width scatter was observed but, because of HF propagation conditions, this was not bordered by low spectral width ionospheric scatter. The DMSP data shows the SWB did not mark a magnetospheric boundary on this occasion. After this time the scatter met our criteria and was associated with either the OCB or the poleward limit of energetic electron precipitation. Clearly, changing propagation conditions are very important and partly explain why SuperDARN radars deployed at different locations tend to observe SWBs under various geophysical conditions.

The October 31 data in particular confirm the SWB was a reasonable proxy for the OCB in the pre-midnight sector during moderately disturbed geomagnetic conditions (Lester et al., 2001; Parkinson et al., 2002). This was shown by a sequence of 9 DMSP satellite passes, including 2 during substorm expansion, 4 during recovery phase. and 3 during a subsequent growth phase. Note that for the first substorms observed on both evenings, the OCB inferred from the SWB tended to contract poleward during the recovery phase. This may represent the arrival of energetic electron precipitation associated with the westward travelling surge, and suggests the effects of nightside reconnection did not prevail in our measurements until after the expansion phase (e.g. Lester et al., 2005). Without simultaneous measurements at many MLTs and modelling the effects of dayside and nightside reconnection rates, we cannot conclude whether our observations favour the near-Earth initiation model of substorm development (Lui, 2001).

The two DMSP passes during the expansion phase of the first substorm on October 31 show the SWB was a proxy for the OCB at least before midnight. However, this result is a tentative one because extrapolating the DMSP boundaries to the MLT of the beam 4 may have large errors during expansion phase when the auroral oval develops complex longitudinal structure. It is also possible the geophysical processes responsible for the large spectral widths penetrate to closed field lines during unstable, substorm conditions. We have not discussed the cause of the large spectral widths, but enhanced ULF wave activity with Pc 1-2 periods in the range 0.1–10 s may contribute to the formation of moderate spectral widths (see André et al., 1999). Initial qualitative assessment of MQI induction magnetometer data recorded during our study intervals suggest that bursts of broadband ULF wave activity were coincident with times when large spectral widths were measured at $-65°\Lambda$.

Observations made during both nights show the SWB changed from being a signature of the OCB before midnight to a signature of some other boundary in the morning sector (>03 MLT), irrespective of substorm phase. An absence of suitable DMSP passes during the early morning hours (~01–03 MLT) prevented us from determining whether there was a gradual or sudden change in the identity of the SWB beyond midnight. However, we speculate the change occurred at ~1500 UT on October 31 when the occurrence of large spectral widths briefly diminished and contracted poleward. It is well known that auroral oval dynamics behave differently in the pre- and post-midnight sectors. For example, more energetic proton precipitation is observed further equatorward post-midnight, and more energetic electron precipitation further equatorward post-midnight. The SWB is actually a better proxy for the poleward limit of energetic electron precipitation, which is often a proxy for the OCB in the pre-midnight sector (Parkinson et al., 2004; Chisham et al., 2005).

The nightside SWB exhibits complex behaviour that we still do not fully understand. For example, the SWB is sometimes bifurcated in full-scan and range-time plots (i.e. not simply because structure in space and time is confused). This bifurcation may arise because of the complicated magnetic field topology arising during current disruption, or because the magnetospheric boundary is a porous surface, as opposed to the smooth surface normally imagined (Lui, 2001). Alternatively, the bifurcation might arise because of spatial and temporal variations in ionospheric Pedersen conductivity (Parkinson et al., 2004). The tendency for spectral widths to sometimes decrease again toward the poleward limit of large spectral width provides for the possibility of another, unobserved SWB located further poleward. Hence, there may be a preference for some SuperDARN radars to observe SWBs located at different latitudes, local times, and IMF and geomagnetic conditions.

The main result of this study is that the TIGER radar tends to observe reproducible expansions and contractions of the nightside SWB which can be reconciled with the spatial and temporal behaviour of energetic particle precipitation throughout the substorm cycle. Our assertions about the MLT and geomagnetic activity behaviour of the SWB were based upon two nights of observations. Clearly, they need more thorough testing using an extensive database of nightside SWB and DMSP OCB identifications sorted according to substorm phase. Nevertheless, we hope the present case studies provide further insights into when the HF radar SWB can be used as a reliable proxy for the OCB, and also aid in the monitoring and prediction of the substorms.

Acknowledgements

This work was supported by the Australian Research Council, the Australian Antarctic Science Advisory Committee, and the Australian Academy of Sciences. The Australian Geological Survey Organisation is thanked for making available MQI fluxgate magnetometer data. P. Wilkinson of the IPS Radio and Space Services, Australia, is thanked for providing Hobart and MQI ionograms. P. Ponomarenko of the University of Newcastle, Australia, is thanked for providing dynamic spectrograms of MQI induction magnetometer data. The DMSP particle detectors were designed by D. Hardy of AFRL, and data obtained from JHU/APL. We thank D. Hardy, F. Rich, and P. Newell for its use. Finally, we thank the numerous people who contributed to the operation of TIGER.

References

André, R., Pinnock, M., Rodger, A.S. On the SuperDARN autocorrelation function observed in the ionospheric cusp. Geophys. Res. Lett. 26, 3353–3356, 1999.

Baker, K.B., Dudeney, J.R., Greenwald, R.A., et al. HF radar signatures of the cusp and low-latitude boundary layer. J. Geophys. Res. 100, 7671–7695, 1995.

Chisham, G., Freeman, M.P. An investigation of latitudinal transitions in the SuperDARN spectral width boundaries and DMSP particle precipitation boundaries in the nightside ionosphere. Geophys. Res. Lett. 31, L02804, doi:10.1029/2003GL019074, 2004.

Chisham, G., Freeman, M.P., Sotirelis, T., et al. A statistical comparison of SuperDARN spectral width boundaries and DMSP particle precipitation boundaries in the morning sector ionosphere. Ann. Geophys. 23, 733–743, 2005.

Dudeney, J.R., Rodger, A.S., Freeman, M.P., Pickett, J., Scudder, J., Sofko, G., Lester, M. The nightside ionospheric response to IMF by changes. Geophys. Res. Lett. 25, 2601–2604, 1998.

Greenwald, R.A. et al. DARN/SuperDARN: A global view of the dynamics of high-latitude convection. Space Sci. Rev. 71, 761–796, 1995.

Lester, M., Milan, S.E., Besser, V., Smith, R. A case study of HF radar spectra and 630.0 nm auroral emission in the pre-midnight sector. Ann. Geophys. 19, 327–339, 2001.

Lester, M., Parkinson, M.L., Wild, J.A., et al. Simultaneous observations of ionospheric flow and tail reconnection signatures during the substorm expansion phase. Ann. Geophysicae, submitted for publication, 2005.

Lui, A.T.Y. Current controversies in magnetospheric physics. Rev. Geophys. 39, 535–563, 2001.

Newell, P.T., Feldstein, Y.I., Galperin, Y.I., Meng, C.-I. Morphology of nightside precipitation. J. Geophys. Res. 101, 10,737–10,748, 1996.

Parkinson, M.L., Dyson, P.L., Pinnock, M., et al. Signatures of the midnight open–closed magnetic field-line boundary during balanced dayside and nightside reconnection. Ann. Geophys. 20, 1617–1630, 2002.

Parkinson, M.L., Chisham, G., Pinnock, M., Dyson, P.L., Devlin, J.C. Magnetic local time, substorm, and particle-precipitation-related variations in the behaviour of SuperDARN Doppler spectral widths. Ann. Geophys. 22, 4103–4122, 2004.

Starkov, G.V. Mathematical model of the auroral boundaries. Geomag. Aeronomy 34, 331–336, 1994.

Vampola, A.L. Access of solar electrons to closed field lines. J. Geophys. Res. 76, 36–43, 1971.